International Journal of Innovative
Computing, Information and Control
Volume 18, Number 1, February 2022
 ISSN 1349-4198
pp. 93–104

FRACTIONAL NON-SINGULAR FAST TERMINAL SLIDING MODE CONTROL BASED ON DISTURBANCE OBSERVER

Xin Zhang[1,2] and Ying Quan[1]

[1]School of Automation and Electrical Engineering
[2]Gansu Provincial Engineering Research Center for Artificial Intelligence and Graphics and Image Processing
Lanzhou Jiaotong University
No. 88, Anning West Road, Anning District, Lanzhou 730070, P. R. China
zhangx@mail.lzjtu.cn; 11200397@stu.lzjtu.edu.cn

Received July 2021; revised November 2021

Abstract. *In order to achieve high-precision tracking control of the manipulator control system, a fractional non-singular fast terminal sliding mode control method based on the disturbance observer is proposed. Firstly, a fractional non-singular fast terminal sliding mode surface is designed according to the theory of fractional calculus to achieve rapid convergence of the trajectory tracking error of the manipulator and improve the tracking performance of the controller; then, the super twisting algorithm is introduced into the sliding mode reaching law and the hyperbolic tangent function reduces the chattering of the control input; and the nonlinear disturbance observer is used to accurately estimate the compound uncertainty disturbance to realize the compensation of the controller; finally, the Lyapunov stability theory is used to prove the stability of the system. Finally, a simulation experiment is carried out with a two-joint manipulator as the research object, and the results verify the effectiveness and robustness of the designed controller.*
Keywords: Manipulator control system, Terminal sliding mode control, Fractional calculus, Super-twisting algorithm, Disturbance observer

1. **Introduction.** With the rapid development of the electronics and mechanical industries, high-performance manipulator systems are widely used in production and life. The manipulator control system is a complex nonlinear system with high coupling and nonlinear characteristics. In order to ensure that the manipulator can safely and stably complete the operation tasks accurately, a high-performance controller is essential. Therefore, how to design a high-performance controller is a research hotspot in the field of manipulator trajectory tracking control.

In view of the trajectory tracking control of the robotic arm, many control methods have been proposed at home and abroad, such as sliding mode control [1-3], adaptive control [4], fuzzy control [5], and neural network control [6]. Sliding mode control is a special kind of nonlinear control, which forms a sliding mode surface according to the current state of the system (such as error and its derivatives). Through the switching of the control quantity, the system is forced to slide along the specified state trajectory to make the system. It is invariant when subjected to uncertain parameters or external interference, and the structure is simple [7,8]. However, the control law used in traditional sliding mode control has a relatively large control gain, which can cause chattering [9]. Therefore, it has certain practical significance to improve the control accuracy of the system while improving the chattering. Since it is difficult to accurately obtain the magnitude of external interference

DOI: 10.24507/ijicic.18.01.93

in actual systems, the introduction of disturbance observers can effectively solve this problem [10].

The sliding mode can be mainly divided into linear sliding mode and nonlinear sliding mode. The ordinary linear sliding mode can make the system gradually converge to the equilibrium point, and the nonlinear sliding mode can make the system state converge to the equilibrium point in a finite time. In [11], an adaptive sliding mode control method based on a disturbance observer is proposed, which improves the system chattering and realizes the precise control of the joint motion of the manipulator. In [12], a new type of variable boundary layer non-singular fast terminal sliding mode control strategy is proposed, which uses the variable boundary layer to weaken chattering and realizes the accurate tracking of permanent magnet synchronous motors. In [13], a super-twisted non-singular sliding mode controller is designed to realize the coordinated control of multiple permanent magnet synchronous motors. However, most of the above-mentioned work uses integer-order control schemes. Fractional calculus is the extension of integral and differential to non-integer-order integral and differential. Compared with integer-order, its process is more delicate and soft, so fractional-order theory is widely used in various industrial projects. In [14], an adaptive fractional-order non-singular fast terminal sliding mode controller is proposed to achieve rapid convergence of the robot system. The simulation results show that the fractional-order controller has better control performance than the integer-order controller. However, the unknown disturbance in the control system has not been properly dealt with. In [15], a fractional-order non-singular terminal sliding mode control method is proposed to achieve accurate tracking and finite-time convergence of the cable manipulator. However, the sliding mode control algorithm used is not advanced enough. In [16], a super distortion algorithm with fractional order integral is proposed to suppress the influence of non-integer order perturbation and dynamic uncertainty and realize the precise control of the electric system. However, the unknown interference in the system is not accurately estimated, and the super-twist algorithm is not used in the robotic arm system.

Inspired by the above-mentioned articles, this paper designs a fractional non-singular fast terminal sliding mode control method based on a nonlinear disturbance observer for the trajectory tracking control problem of the manipulator, which combines the super-twist algorithm with the hyperbolic tangent function to form a sliding control method. Mode reaching law can effectively reduce chattering, fractional non-singular fast terminal sliding mode surfaces can achieve rapid system convergence, and nonlinear disturbance observers can estimate uncertain disturbance to achieve system input compensation. Through simulation experiment comparison with other control methods, the accuracy and effectiveness of the designed controller for the trajectory tracking of the manipulator are verified.

The specific contributions of this paper are as follows.

1) In this paper, a fractional-order non-singular fast terminal sliding mode surface is designed to improve the convergence accuracy and speed of the system state in the sliding mode.

2) The super-twisting algorithm improves the performance of the system state in the approaching mode, and accelerates the speed of the system state approaching the sliding mode surface.

3) This paper introduces a disturbance observer to accurately estimate the external disturbance in the system, and further improves the accuracy of the manipulator control system.

4) The stability of the control system is proved by the Lyapunov function.

The rest of the paper is arranged as follows. The second section introduces the basic theory of fractional order and the dynamic model of the manipulator. The third section introduces the control scheme designed in this paper, the fourth section carries on the simulation analysis, and the fifth section is the conclusion part.

2. Mathematical Preliminaries.

2.1. **The basic theory of fractional order.** At present, there are three definitions of fractional calculus that are widely used in the control field, namely: Grunwald-Letnikov (GL) definition, Riemann-Liouville (RL) definition and Caputo definition [17]. The definition of the initial conditions of Caputo-type fractional calculus is consistent with that of integer-order calculus and has been extensively studied in engineering applications in recent years.

The definition of Caputo-type fractional calculus is as follows [18]:

$$ {}_aD_t^{\alpha} f(t) = \frac{1}{\Gamma(m-\alpha)} \int_a^t \frac{f^{(m)}(\sigma)}{(t-\sigma)^{\alpha-m+1}} d\sigma, \quad m-1 < \alpha \le m \tag{1}$$

where ${}_aD_t^{\alpha}$ is the fractional calculus operator, where a and t represent the lower limit and upper limit of the fractional calculus operator, respectively, and α is the order of the fractional calculus operator. To simplify the expression, use ${}_aD_t^{\alpha}$ instead of D^{α}. m is the smallest integer greater than α, and $\Gamma(.)$ is the Gamma function.

Lemma 2.1. [19]*:*

$$D^{\alpha} x(t) = f(x,t) \tag{2}$$

If it is the equilibrium point of the non-autonomous fractional-order system, it satisfies the Lipschitz condition. Suppose there is a Lyapunov function that satisfies the following conditions:

$$\alpha_1 \|x\| \le V(t,x) \le \alpha_2 \|x\|, \quad \dot{V}(t,x) \le -\alpha_3 \|x\| \tag{3}$$

where α_1, α_2 and α_3 are all normal numbers, $\beta \in (0,1)$. Then the system (2) is progressively stable.

2.2. **Dynamics model of the manipulator.** For the n-joint rigid manipulator, according to the Lagrange equation, its dynamic model is expressed as

$$\boldsymbol{M}(\boldsymbol{q})\ddot{\boldsymbol{q}} + \boldsymbol{C}(\boldsymbol{q},\dot{\boldsymbol{q}})\dot{\boldsymbol{q}} + \boldsymbol{G}(\boldsymbol{q}) = \boldsymbol{\tau} \tag{4}$$

where $\boldsymbol{q} \in \boldsymbol{R}^n$ is the joint position, $\dot{\boldsymbol{q}} \in \boldsymbol{R}^n$ and $\ddot{\boldsymbol{q}} \in \boldsymbol{R}^n$ are the velocity vector and acceleration vector, $\boldsymbol{M}(\boldsymbol{q}) \in \boldsymbol{R}^{n\times n}$ is the inertia matrix, $\boldsymbol{C}(\boldsymbol{q},\dot{\boldsymbol{q}}) \in \boldsymbol{R}^{n\times n}$ is the centrifugal force and Coriolis force matrix, $\boldsymbol{G}(\boldsymbol{q}) \in \boldsymbol{R}^n$ is the gravity term, and $\boldsymbol{\tau} \in \boldsymbol{R}^n$ is the control moment.

In practical applications, due to the influence of external environmental noise and measurement errors, $\boldsymbol{M}(\boldsymbol{q})$, $\boldsymbol{C}(\boldsymbol{q},\dot{\boldsymbol{q}})$ and $\boldsymbol{G}(\boldsymbol{q})$ are not easy to obtain. Considering the uncertainty of the parameters, the above parameters are divided into nominal values and disturbance values:

$$\boldsymbol{M}(\boldsymbol{q}) = \boldsymbol{M}_0(\boldsymbol{q}) + \Delta\boldsymbol{M}(\boldsymbol{q}) \tag{5}$$

$$\boldsymbol{C}(\boldsymbol{q},\dot{\boldsymbol{q}}) = \boldsymbol{C}_0(\boldsymbol{q},\dot{\boldsymbol{q}}) + \Delta\boldsymbol{C}(\boldsymbol{q},\dot{\boldsymbol{q}}) \tag{6}$$

$$\boldsymbol{G}(\boldsymbol{q}) = \boldsymbol{G}_0(\boldsymbol{q}) + \Delta\boldsymbol{G}(\boldsymbol{q}) \tag{7}$$

where $\boldsymbol{M}_0(\boldsymbol{q})$, $\boldsymbol{C}_0(\boldsymbol{q},\dot{\boldsymbol{q}})$, $\boldsymbol{G}_0(\boldsymbol{q})$ are nominal values; $\Delta\boldsymbol{M}(\boldsymbol{q})$, $\Delta\boldsymbol{C}(\boldsymbol{q},\dot{\boldsymbol{q}})$, $\Delta\boldsymbol{G}(\boldsymbol{q})$ are disturbance values.

Regarding system modeling errors, parameter changes and other uncertain factors as external disturbances, expressed by $\boldsymbol{\tau}_{\mathrm{d}}$, (4) becomes

$$\boldsymbol{M}_0(\boldsymbol{q})\ddot{\boldsymbol{q}} + \boldsymbol{C}_0(\boldsymbol{q},\dot{\boldsymbol{q}})\dot{\boldsymbol{q}} + \boldsymbol{G}_0(\boldsymbol{q}) = \boldsymbol{\tau} + \boldsymbol{\tau}_{\mathrm{d}} \tag{8}$$

3. Design of Manipulator Control System.

3.1. Design of sliding controller. According to the dynamic model of the manipulator, $\boldsymbol{q}_{\mathrm{d}}(t)$ is defined as the ideal position of the joint and $\boldsymbol{q}(t)$ is the actual position of the joint. The position tracking error of each joint of the manipulator is defined as

$$\boldsymbol{e}(t) = \boldsymbol{q}_{\mathrm{d}}(t) - \boldsymbol{q}(t) \tag{9}$$

Take the second derivative of (9):

$$\ddot{\boldsymbol{e}} = \ddot{\boldsymbol{q}}_{\mathrm{d}} - \ddot{\boldsymbol{q}} \tag{10}$$

The non-singular fast terminal sliding surface in [20] is

$$\boldsymbol{s} = \boldsymbol{e} + \lambda \left|\dot{\boldsymbol{e}}\right|^{\gamma} \operatorname{sign}\left(\dot{\boldsymbol{e}}\right) \tag{11}$$

where λ is a system parameter and γ is a normal number. However, there is still room for improvement in the convergence speed and control accuracy of the sliding surface.

To design a controller to improve the trajectory tracking effect of the manipulator system, a class of fractional non-singular fast terminal sliding surface is defined as

$$\boldsymbol{s} = D^{\alpha}\boldsymbol{e} + a \cdot \boldsymbol{e} + b \cdot \left|\boldsymbol{e}\right|^{\frac{q}{p}} \operatorname{sign}\left(\boldsymbol{e}\right) \tag{12}$$

where $\alpha \in (0, 1)$ is a real number, a and b are normal numbers, p and q are all positive odd numbers, $1 < q/p < 2$.

Ensure that the exponent of the error $\boldsymbol{e}$ in the sliding mode surface function $\boldsymbol{s}$ is greater than 1, which can avoid the error exponent being negative after deriving and ensure the non-singularity of the sliding mode surface [21].

Take the derivative of (12):

$$\dot{\boldsymbol{s}} = D^{\alpha-1}\ddot{\boldsymbol{e}} + a \cdot \dot{\boldsymbol{e}} + b \cdot \frac{q}{p} \cdot \left|\boldsymbol{e}\right|^{\frac{q}{p}-1} \cdot \dot{\boldsymbol{e}} \cdot \operatorname{sign}(\boldsymbol{e}) \tag{13}$$

Since the sliding mode function needs to switch continuously in the sliding mode surface, the sliding mode control algorithm will have chattering near the equilibrium point. For a common sliding mode approaching law such as $-\varepsilon\operatorname{sign}(\boldsymbol{s})$, the approaching speed is finite and contains a sign function. The high-order sliding mode algorithm applies the sign function to the high-order derivative of the sliding mode variable, which can effectively suppress chattering [22]. The super-twist algorithm is a high-order sliding mode algorithm, which only needs sliding mode variables, so that the sliding mode variables are hidden in the high-order derivatives, which can effectively avoid chattering and help simplify the controller structure. Through the super twisting nonlinear equation, the sliding mode reaching law can be obtained as

$$\dot{\boldsymbol{s}} = -k_1 \left|\boldsymbol{s}\right|^{\frac{1}{2}} \operatorname{sign}(\boldsymbol{s}) - \int_0^t k_2 \operatorname{sign}(\boldsymbol{s})\mathrm{d}t - k_3\boldsymbol{s} \tag{14}$$

where k_1, k_2 and k_3 are switching gains.

In Equation (14), the discontinuous sign function intensifies the chattering in the sliding mode control process, the hyperbolic tangent function is used instead of the sign function, and the smoothness of this function is used to greatly alleviate the degree of control signal switching chattering. The hyperbolic tangent function is defined as

$$\tanh(x) = \frac{\mathrm{e}^x - \mathrm{e}^{-x}}{\mathrm{e}^x + \mathrm{e}^{-x}} \tag{15}$$

where e is a natural constant.

The sliding mode reaching law based on the hyperbolic tangent function is as follows:

$$\dot{\boldsymbol{s}} = -k_1 \left|\boldsymbol{s}\right|^{\frac{1}{2}} \tanh(\boldsymbol{s}) - \int_0^t k_2 \tanh(\boldsymbol{s}) \mathrm{d}t - k_3 \boldsymbol{s} \tag{16}$$

From (13) and (16), the control law is

$$\begin{aligned}\boldsymbol{\tau} = \boldsymbol{M}_0 \Bigg(\ddot{\boldsymbol{q}}_\mathrm{d} + D^{1-\alpha} \Bigg(k_1 |\boldsymbol{s}|^{\frac{1}{2}} \tanh(\boldsymbol{s}) + \int_0^t k_2 \tanh(\boldsymbol{s}) \mathrm{d}t + k_3 \boldsymbol{s} + a \cdot \dot{\boldsymbol{e}} \\ + b \cdot \frac{q}{p} \cdot |\boldsymbol{e}|^{\frac{q}{p}-1} \cdot \dot{\boldsymbol{e}} \cdot \mathrm{sign}(\boldsymbol{e}) \Bigg) \Bigg) + \boldsymbol{C}_0 \dot{\boldsymbol{q}} + \boldsymbol{G}_0 - \boldsymbol{\tau}_\mathrm{d}\end{aligned} \tag{17}$$

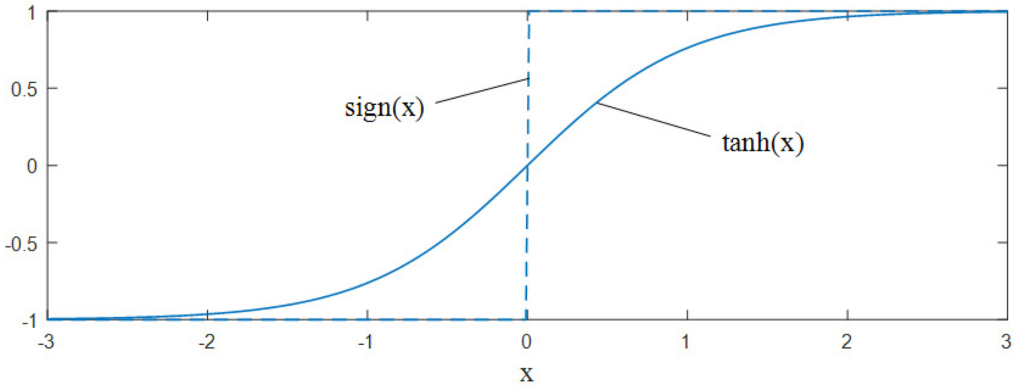

FIGURE 1. Curve comparison between hyperbolic tangent function and symbolic function

3.2. **Design of nonlinear disturbance observer.** In actual engineering, the composite disturbance $\boldsymbol{\tau}_\mathrm{d}$ is usually difficult to obtain and needs to be estimated, but there is a certain error between the estimated value of the disturbance and the actual value. The basic idea of disturbance observer design is to use the difference between the estimated output and the actual output to correct the estimated value to achieve the effect of suppressing disturbance and enhance the robustness of the system to disturbance. $\hat{\boldsymbol{\tau}}_\mathrm{d}$ represents the estimation of disturbance $\boldsymbol{\tau}_\mathrm{d}$, and the nonlinear disturbance observer is designed as

$$\begin{cases} \dot{\boldsymbol{z}} = -\boldsymbol{L}(\boldsymbol{q}, \dot{\boldsymbol{q}}) \boldsymbol{z} + \boldsymbol{L}(\boldsymbol{q}, \dot{\boldsymbol{q}}) (\boldsymbol{C}_0 (\boldsymbol{q}, \dot{\boldsymbol{q}}) \dot{\boldsymbol{q}} + \boldsymbol{G}_0 (\boldsymbol{q}) - \boldsymbol{\tau} - \boldsymbol{p}(\boldsymbol{q}, \dot{\boldsymbol{q}})) \\ \hat{\boldsymbol{\tau}}_\mathrm{d} = \boldsymbol{z} + \boldsymbol{p}(\boldsymbol{q}, \dot{\boldsymbol{q}}) \end{cases} \tag{18}$$

where $\boldsymbol{z}$ is the defined auxiliary variable; $\boldsymbol{p}(\boldsymbol{q}, \dot{\boldsymbol{q}})$ is the nonlinear function to be designed; $\boldsymbol{L}(\boldsymbol{q}, \dot{\boldsymbol{q}})$ is the gain of the nonlinear observer, which satisfies the following conditions:

$$\boldsymbol{L}(\boldsymbol{q}, \dot{\boldsymbol{q}}) \boldsymbol{M}_0 (\boldsymbol{q}) \ddot{\boldsymbol{q}} = \frac{\mathrm{d}\boldsymbol{p}(\boldsymbol{q}, \dot{\boldsymbol{q}})}{\mathrm{d}\boldsymbol{t}} \tag{19}$$

The observation error $\boldsymbol{f}$ of the nonlinear disturbance observer is defined as

$$\boldsymbol{f} = \boldsymbol{\tau}_\mathrm{d} - \hat{\boldsymbol{\tau}}_\mathrm{d} \tag{20}$$

Assume that the disturbance changes slowly relative to the dynamic characteristics of the interference observer, that is

$$\dot{\boldsymbol{\tau}}_\mathrm{d} = 0 \tag{21}$$

According to (19) and (21), the dynamic equation of the observer can be obtained as

$$\dot{\boldsymbol{f}} = \dot{\boldsymbol{\tau}}_\mathrm{d} - \dot{\hat{\boldsymbol{\tau}}}_\mathrm{d} = -\dot{\hat{\boldsymbol{\tau}}}_\mathrm{d} = -\dot{\boldsymbol{z}} - \frac{\mathrm{d}\boldsymbol{p}(\boldsymbol{q}, \dot{\boldsymbol{q}})}{\mathrm{d}\boldsymbol{t}} \tag{22}$$

Substituting (18) and (19) into Formula (22), we can get

$$\dot{\boldsymbol{f}} = \boldsymbol{L}\left(\boldsymbol{q},\dot{\boldsymbol{q}}\right)\left(\boldsymbol{z}+\boldsymbol{p}\left(\boldsymbol{q},\dot{\boldsymbol{q}}\right)\right) - \boldsymbol{L}\left(\boldsymbol{q},\dot{\boldsymbol{q}}\right)\left(\boldsymbol{M}_0(\boldsymbol{q})\ddot{\boldsymbol{q}} + \boldsymbol{C}_0\left(\boldsymbol{q},\dot{\boldsymbol{q}}\right)\dot{\boldsymbol{q}} + \boldsymbol{G}_0(\boldsymbol{q}) - \boldsymbol{\tau}\right) \tag{23}$$

Combining (8) and (18), (23) can be changed to

$$\dot{\boldsymbol{f}} = \boldsymbol{L}\left(\boldsymbol{q},\dot{\boldsymbol{q}}\right)\hat{\boldsymbol{\tau}}_{\mathrm{d}} - \boldsymbol{L}\left(\boldsymbol{q},\dot{\boldsymbol{q}}\right)\boldsymbol{\tau}_{\mathrm{d}} = -\boldsymbol{L}\left(\boldsymbol{q},\dot{\boldsymbol{q}}\right)\boldsymbol{f} \tag{24}$$

Obtain the dynamic equation of the observer error system as

$$\dot{\boldsymbol{f}} + \boldsymbol{L}\left(\boldsymbol{q},\dot{\boldsymbol{q}}\right)\boldsymbol{f} = 0 \tag{25}$$

Design matrix $\boldsymbol{L}\left(\boldsymbol{q},\dot{\boldsymbol{q}}\right) = \mathrm{diag}\{c,c\}$, $c>0$.

Choose the Lyapunov function

$$V_1 = \frac{1}{2}\boldsymbol{f}^{\mathrm{T}}\boldsymbol{f} \tag{26}$$

Taking the derivation of (26):

$$\dot{V}_1 = \boldsymbol{f}^{\mathrm{T}}\dot{\boldsymbol{f}} = -\boldsymbol{f}^{\mathrm{T}}\boldsymbol{L}\left(\boldsymbol{q},\dot{\boldsymbol{q}}\right)\boldsymbol{f} \le 0 \tag{27}$$

therefore, the disturbance estimation error gradually converges.

The control law becomes

$$\begin{aligned}\boldsymbol{\tau} = \boldsymbol{M}_0\Bigg(\ddot{\boldsymbol{q}}_{\mathrm{d}} + D^{1-\alpha}\Bigg(&k_1\left|\boldsymbol{s}\right|^{\frac{1}{2}}\tanh(\boldsymbol{s}) + \int_0^t k_2\tanh(\boldsymbol{s})\mathrm{d}t + k_3\boldsymbol{s} + a\cdot\dot{\boldsymbol{e}}\\ &+ b\cdot\frac{q}{p}\cdot|\boldsymbol{e}|^{\frac{q}{p}-1}\cdot\dot{\boldsymbol{e}}\cdot\mathrm{sign}(\boldsymbol{e})\Bigg)\Bigg) + \boldsymbol{C}_0\dot{\boldsymbol{q}} + \boldsymbol{G}_0 - \hat{\boldsymbol{\tau}}_{\mathrm{d}}\end{aligned} \tag{28}$$

3.3. **Stability analysis.** Select the Lyapunov function

$$V = V_1 + \frac{1}{2}\boldsymbol{s}^2 \tag{29}$$

It can be seen that (29) is greater than zero. According to Formula (27), $\dot{V}_1 \le 0$, the derivative of (29) can be obtained

$$\begin{aligned}\dot{V} &= \dot{V}_1 + \boldsymbol{s}\cdot\dot{\boldsymbol{s}}\\ &= \dot{V}_1 + \boldsymbol{s}\cdot\left(D^{\alpha-1}\ddot{\boldsymbol{e}} + a\cdot\dot{\boldsymbol{e}} + b\cdot\frac{q}{p}\cdot|\boldsymbol{e}|^{\frac{q}{p}-1}\cdot\dot{\boldsymbol{e}}\cdot\mathrm{sign}(\boldsymbol{e})\right)\\ &= \dot{V}_1 + \boldsymbol{s}\cdot\left(-k_1\left|\boldsymbol{s}\right|^{\frac{1}{2}}\tanh(\boldsymbol{s}) - \int_0^t k_2\tanh(\boldsymbol{s})\mathrm{d}t - k_3\boldsymbol{s}\right)\\ &\le 0\end{aligned} \tag{30}$$

According to the Lyapunov stability criterion, the system can be judged to be asymptotically stable.

4. **Simulation Results.**

Taking the two-joint manipulator as an example, MATLAB is used to simulate the system. Use FOMCON's fractional-order modeling and control toolbox to complete the numerical simulation. According to the aforementioned dynamic model of the robotic arm system, its specific parameters are as follows:

$$\boldsymbol{M}(\boldsymbol{q}) = \begin{bmatrix} v + q_{01} + 2q_{02}\cos(q_2) & q_{01} + q_{02}\cos(q_2)\\ q_{01} + q_{02}\cos(q_2) & q_{01}\end{bmatrix}$$

$$\boldsymbol{C}(\boldsymbol{q},\dot{\boldsymbol{q}}) = \begin{bmatrix} -q_{02}\dot{q}_2\sin(q_2) & -q_{02}(\dot{q}_1+\dot{q}_2)\sin(q_2)\\ q_{02}\dot{q}_1\sin(q_2) & 0\end{bmatrix}$$

$$\boldsymbol{G}(\boldsymbol{q}) = \begin{bmatrix} 15g\cos q_1 + 8.75g\cos(q_1+q_2) \\ 8.75g\cos(q_1+q_2) \end{bmatrix}$$
$$\boldsymbol{\tau}_{\mathrm{d}} = 3\sin(2\pi t)$$

where $v = 13.33$, $q_{01} = 8.98$, $q_{02} = 8.75$, $g = 9.8$. The two joint position commands are $q_{1\mathrm{d}} = \cos(\pi t)$, $q_{2\mathrm{d}} = \sin(\pi t)$. The initial state of the two-joint manipulator system is given as $[q_1 \quad q_2 \quad q_3 \quad q_4] = [0 \quad 3 \quad 1 \quad 0]$.

In order to reflect the superiority of the controller in this paper, the following three control methods are used for simulation comparison and analysis. Compared with the method proposed in this paper, the method 2 uses the sliding surface in [20], and the method 3 uses the sliding mode approaching law in [13]:

Method 1:

$$\begin{aligned}\boldsymbol{\tau} = \boldsymbol{M}_0\Bigg(\ddot{\boldsymbol{q}}_{\mathrm{d}} + D^{1-\alpha}\Bigg(k_1\left|\boldsymbol{s}\right|^{\frac{1}{2}}\tanh(\boldsymbol{s}) + \int_0^t k_2\tanh(\boldsymbol{s})\mathrm{d}t + k_3\boldsymbol{s} + a\cdot\dot{\boldsymbol{e}} \\ + b\cdot\frac{q}{p}\cdot\left|\boldsymbol{e}\right|^{\frac{q}{p}-1}\cdot\dot{\boldsymbol{e}}\cdot\mathrm{sign}(\boldsymbol{e})\Bigg)\Bigg) + \boldsymbol{C}_0\dot{\boldsymbol{q}} + \boldsymbol{G}_0 - \hat{\boldsymbol{\tau}}_{\mathrm{d}}\end{aligned} \tag{31}$$

Method 2:

$$\begin{aligned}\boldsymbol{\tau} = \boldsymbol{M}_0\left(\ddot{\boldsymbol{q}}_{\mathrm{d}} + \frac{1}{\lambda\gamma}\left|\dot{\boldsymbol{e}}\right|^{2-\gamma}\mathrm{sign}(\dot{\boldsymbol{e}}) + k_1\left|\boldsymbol{s}\right|^{\frac{1}{2}}\tanh(\boldsymbol{s}) + \int_0^t k_2\tanh(\boldsymbol{s})\mathrm{d}t + k_3\boldsymbol{s}\right) \\ + \boldsymbol{C}_0\dot{\boldsymbol{q}} + \boldsymbol{G}_0 - \hat{\boldsymbol{\tau}}_{\mathrm{d}}\end{aligned} \tag{32}$$

Method 3:

$$\begin{aligned}\boldsymbol{\tau} = \boldsymbol{M}_0\Bigg(\ddot{\boldsymbol{q}}_{\mathrm{d}} + D^{1-\alpha}\Bigg(k_1\left|\boldsymbol{s}\right|^{\frac{1}{2}}\tanh(\boldsymbol{s}) + \int_0^t k_2\tanh(\boldsymbol{s})\mathrm{d}t + a\cdot\dot{\boldsymbol{e}} \\ + b\cdot\frac{q}{p}\cdot\left|\boldsymbol{e}\right|^{\frac{q}{p}-1}\cdot\dot{\boldsymbol{e}}\cdot\mathrm{sign}(\boldsymbol{e})\Bigg)\Bigg) + \boldsymbol{C}_0\dot{\boldsymbol{q}} + \boldsymbol{G}_0 - \hat{\boldsymbol{\tau}}_{\mathrm{d}}\end{aligned} \tag{33}$$

In order to reflect the superior performance of the controller, through a large number of simulation experiments, the control parameters are set as $a = 60$, $b = 5$, $p = 3$, $q = 5$, $\alpha = 0.1$, $k_1 = 15$, $k_2 = 30$, $k_3 = 3$, $\gamma = 1.5$, $\lambda = 0.8$.

Figure 2 shows the position tracking situation of the three control methods. All three methods can achieve relatively effective tracking. Method 1 can basically track the command trajectory in about 0.5 seconds, but method 2 and method 3 are basically completely track the instruction trajectory at around 1.3 seconds and 2 seconds. After comparing and analyzing the enlarged view of the tracking curve, it can be seen that the tracking effect of method 1 is better than that of method 2 and method 3, and its tracking performance is better.

Figure 3 shows the comparison of the position error convergence of the manipulator of the three methods. It can be seen that the error convergence rate of the method 1 is faster than that of the method 2 and method 3. In order to analyze the performance of the control method more clearly, the root mean square error of the angular displacement adjustment time and position error are selected as the judgment reference value. Angular displacement adjustment time refers to the time it takes for the angular displacement to change from the initial state to the tracking error less than or equal to 0.01 rad. The root mean square error can reflect the deviation between the observed value and the true value to realize the judgment of the following performance. According to the simulation data analysis, Table 1 is obtained. Analyze the data in the table. It can be seen that the tracking speed and tracking effect of method 1 are better than that of method 2 and method 3.

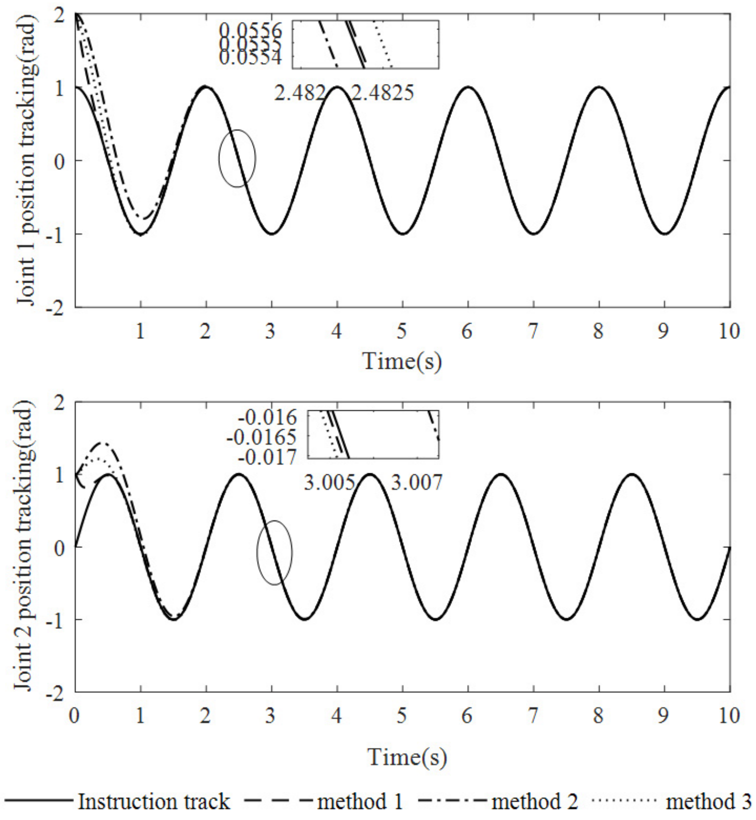

FIGURE 2. Position tracking of joint 1 and joint 2

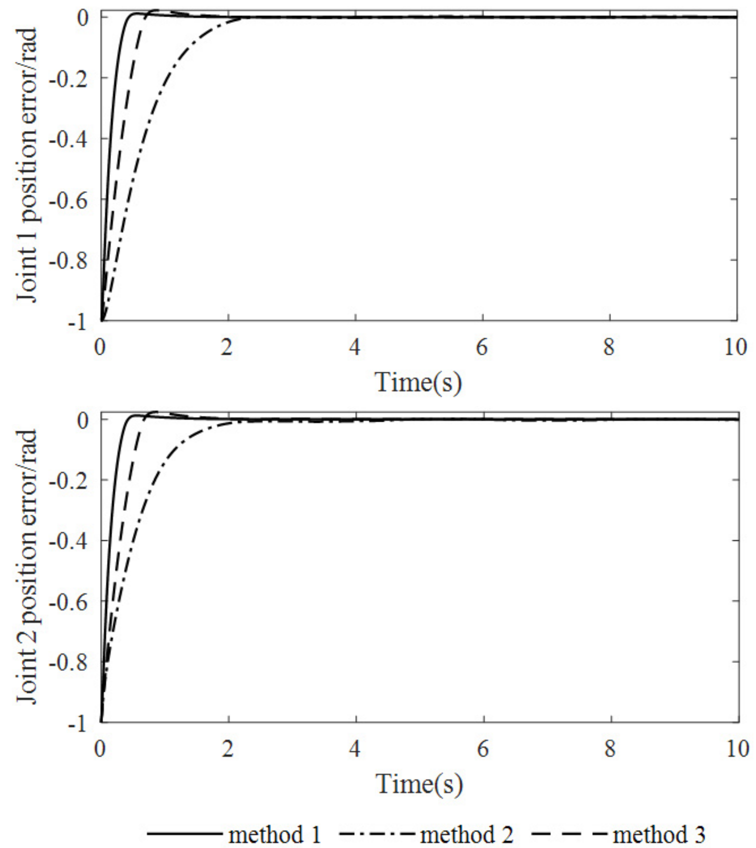

FIGURE 3. Convergence of position error of joint 1 and joint 2

TABLE 1. Data comparison of method 1, method 2 and method 3

	Method 1	Method 2	Method 3
Joint 1 angular displacement adjustment time(s)	0.41	2.11	1.32
Joint 2 angular displacement adjustment time(s)	0.39	2.13	1.35
Root mean square error of joint 1 position error after 2s (rad)	2.66×10^{-5}	2.52×10^{-3}	1.69×10^{-4}
Root mean square error of joint 2 position error after 2s (rad)	8.86×10^{-5}	3.11×10^{-3}	1.71×10^{-4}

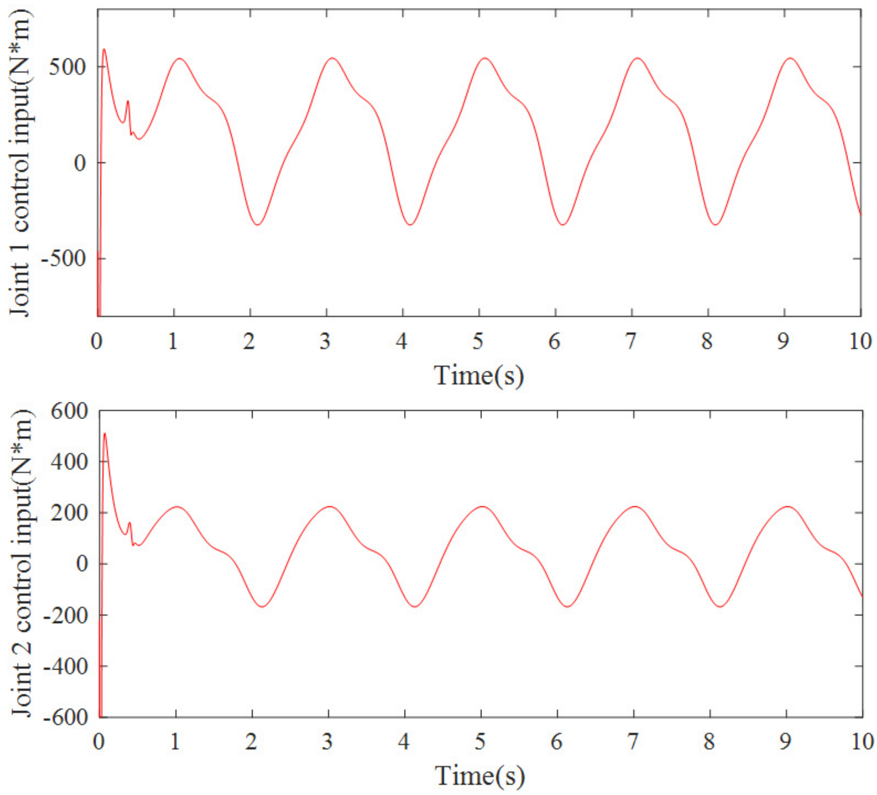

FIGURE 4. Control input of method 1

Figure 4 and Figure 5 show the system control input curve and disturbance estimation curve of method one, respectively. It can be seen that method 1 has a good suppression effect on chattering, and the control input signal produced is relatively smooth. The nonlinear disturbance observer has a good effect on the disturbance, and the estimate is more accurate.

5. **Conclusions.** In order to improve the control performance of the industrial manipulator system, this paper designs a fractional-order non-singular fast terminal sliding mode controller based on the disturbance observer based on the dynamic model of the manipulator. The controller is mainly divided into three parts. First, a fractional-order non-singular fast terminal sliding surface is designed to improve the speed and accuracy of the system state converging to the equilibrium point. Secondly, a super-twisting algorithm is designed in the approaching stage of sliding mode control, which improves the performance of the system state in the approaching mode. At the same time, the nonlinear disturbance observer is used to accurately estimate the size of the external disturbance, which further improves the accuracy of the manipulator control system. Finally,

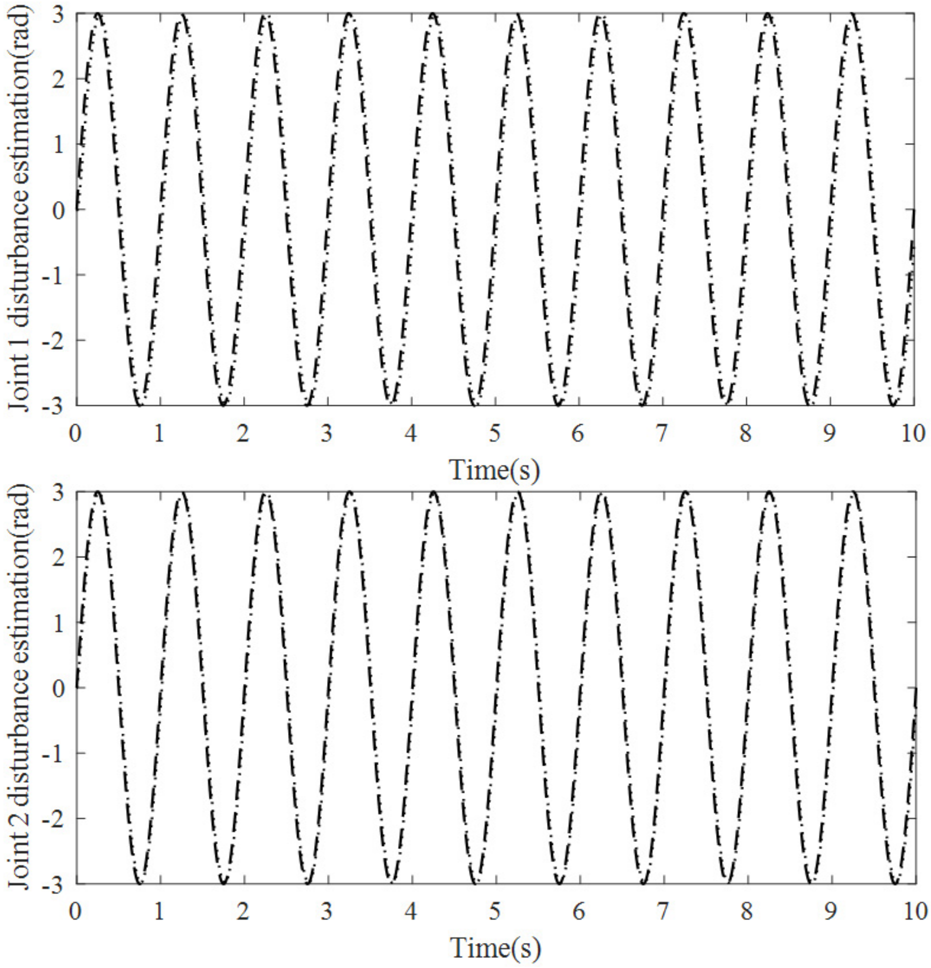

FIGURE 5. Disturbance estimation of joint 1 and joint 2

the stability of the control system is proved by the Lyapunov function, and the simulation analysis results show that under the action of the control method proposed in this paper, the system state convergence speed and tracking accuracy are better than the other two methods, which proves the superiority and effectiveness of the controller designed in this paper. The simulation results show that the controller proposed in this paper reduces the root mean square error of the position error of the two joints to a certain extent. Compared with the other two methods, the root mean square error of the position error of joint one is reduced by 2.49×10^{-3} rad and 1.43×10^{-4} rad, and the root mean square error of the position error of joint two is reduced by 3.03×10^{-3} rad, 8.24×10^{-5} rad. In the future, the effectiveness of the control scheme designed in this paper will be further verified in actual projects.

Acknowledgment. This work is partially supported by the Natural Science Foundation of Gansu Province (No. 20JR5RA419), Lanzhou Jiaotong University-Tianjin University Innovation Fund Project (No. 2019053). The authors also gratefully acknowledge the helpful comments and suggestions of the reviewers, which have improved the presentation.

REFERENCES

[1] A. T. Azar, F. E. Serrano, S. Vaidyanathan and H. Albalawi, Adaptive higher order sliding mode control for robotic manipulators with matched and mismatched uncertainties, *Advances in Intelligent Systems and Computing*, vol.921, pp.360-369, 2020.

[2] D. Matouk, F. Abdessemed, O. Gherouat and Y. Terchi, Second-order sliding mode for positionand attitude tracking control of quadcopter UAV: Super-twisting algorithm, *International Journal of Innovative Computing, Information and Control*, vol.16, no.1, pp.29-43, 2020.
[3] D. M. Huang, L. J. Han, G. Y. Tang, Z. C. Zhou and G. H. Xu, Fractional integral sliding mode control for trajectory tracking of underwater manipulators, *China Mechanical Engineering*, vol.30, no.13, pp.1513-1518, 2019.
[4] D. Wang, H. B. He and D. R. Liu, Adaptive critic nonlinear robust control: A survey, *IEEE Trans. Cybernetics*, vol.47, no.10, pp.3429-3451, 2017.
[5] M. Wang, G. R. Bian and H. S. Li, A new fuzzy iterative learning control algorithm for single joint manipulator, *Archives of Control Sciences*, vol.26, no.3, pp.297-310, 2016.
[6] F. J. Luan, J. Na, Y. B. Huang and G. B. Gao, Adaptive neural network control for robotic manipulators with guaranteed finite-time convergence, *Neurocomputing*, vol.337, pp.153-164, 2019.
[7] Y. X. Su and C. H. Zheng, A new nonsingular integral terminal sliding mode control for robot manipulators, *International Journal of Systems Science*, vol.51, no.8, pp.1418-1428, 2020.
[8] J. K. Liu and F. C. Sun, Research and development on theory and algorithms of sliding mode control, *Control Theory and Applications*, vol.24, no.3, pp.407-418, 2007.
[9] H. Zhang, H. Y. Dong, B. P. Zhang, T. Wu and C. W. Chen, Research on beam supply control strategy based on sliding mode control, *Archives of Electrical Engineering*, vol.69, no.2, pp.349-364, 2020.
[10] L. Zhang, M. Chen and B. Wu, Observer-based controller design for networked control systems with induced delays and data packet dropouts, *ICIC Express Letters, Part B: Applications*, vol.12, no.3, pp.243-253, 2021.
[11] B. B. Zhang, D. Y. Zhao and T. Zhao, Adaptive sliding mode control based on disturbance observer for manipulator systems, *Information and Control*, vol.47, no.2, pp.184-190+199, 2018.
[12] X. J. Chang, L. Liu and R. X. Cui, A nonsingular fast terminal sliding mode controller with varying boundary layers for permanent magnet synchronous motors, *Journal of Xi'an Jiaotong University*, vol.49, no.6, pp.53-59, 2015.
[13] J. Wang, T. T. Jin and J. Zhang, Multi-motor coordination control based on super-twisting nonsingular sliding mode, *Science Technology and Engineering*, vol.20, no.8, pp.3257-3262, 2020.
[14] D. Nojavanzadeh and M. Badamchizadeh, Adaptive fractional-order non-singular fast terminal sliding mode control for robot manipulators, *IET Control Theory & Applications*, vol.10, no.13, pp.1565-1572, 2016.
[15] Y. Y. Wang, S. R. Jiang, B. Chen and H. T. Wu, A new continuous fractional-order nonsingular terminal sliding mode control for cable-driven manipulators, *Advances in Engineering Software*, vol.119, pp.21-29, 2018.
[16] A. J. Muñoz-Vázquez, J. D. Sánchez-Torres, V. Parra-Vega, A. Sánchez-Orta and F. Martínez-Reyes, A fractional super-twisting control of electrically driven mechanical systems, *Transactions of the Institute of Measurement and Control*, vol.42, no.3, pp.485-492, 2020.
[17] H. T. Yu and B. Shi, Analysis and design of fractional sliding mode control for nonlinear systems, *Journal of Naval Aeronautical and Astronautical University*, vol.31, no.4, pp.407-414+422, 2016.
[18] H. Delavari, D. Baleanu and J. Sadati, Stability analysis of caputo fractional-order nonlinear systems revisited, *Nonlinear Dynamics*, vol.67, no.4, pp.2433-2439, 2012.
[19] S. Dadras and H. R. Momeni, Fractional terminal sliding mode control design for a class of dynamical systems with uncertainty, *Communications in Nonlinear Science and Numerical Simulation*, vol.17, no.1, pp.367-377, 2011.
[20] W. Wang, J. T. Zhao, K. R. Hu and Y. C. Guo, Tracking method of manipulator arm based on fast non-singular terminal sliding mode, *Journal of Jilin University (Engineering and Technology Edition)*, vol.50, no.2, pp.464-471, 2020.
[21] X. N. Chi and K. Zhou, Multi-motor synchronous control method for shaft-less drive system, *Journal of Mechanical & Electrical Engineering*, vol.36, no.4, pp.397-401, 2019.
[22] Z. G. Song, C. L. Xia, Z. Q. Wang and T. N. Shi, Direct torque control for permanent magnet synchronous motor using super twisting algorithm, *Transactions of China Electrotechnical Society*, vol.32, no.15, pp.89-99, 2017.

Author Biography

Xin Zhang Ph.D., is an associate professor at School of Automation & Electrical Engineering, Lanzhou Jiaotong University, mainly engaged in intelligent control, design of embedded system. Dr. Zhang obtained the bachelor degree of automation specialty in the Lanzhou Railway Institute in June 2002, obtained the master degree of control engineering and theory in the Lanzhou Jiaotong University in June 2009 and obtained the doctor degree in traffic information engineering and control from Lanzhou Jiaotong University in June 2018.

Ying Quan is a Master's degree student. Her main research direction is industrial robot control. Ms. Quan received a bachelor's degree in intelligent science and technology from Xi'an University of Posts and Telecommunications in June 2020.